Review

Prabhakar R. Bandaru*, Hidenori Yamada, Rajaram Narayanan and Mark Hoefer

The role of defects and dimensionality in influencing the charge, capacitance, and energy storage of graphene and 2D materials

Abstract: The inevitable presence of defects in graphene and other two-dimensional (2D) materials influences the charge density and distribution along with the concomitant measured capacitance and the related energy density. We review, in this paper, the various manifestations of the capacitance including both the classical electrostatic (e.g. associated with double layer, space charge, chemical capacitances) and the quantum forms, as well as a few methodologies to tune the respective capacitances. The role of a proper determination of the surface area of 2D materials, considering the presence of defects, in determining the capacitance and the magnitude of the energy storage is also considered.

Keywords: 2D materials; capacitance; defects; energy storage; graphene.

1 Introduction

The past few decades have witnessed the considerable progress into exploring the scientific aspects of probing materials at the nanometer scale and the consequent impact on ushering new and improved technology. Considering that the harness and storage of energy have been considered the major problem of humanity [1], it would be natural to consider the role that nanostructures could play in solving the problem. At the very outset, the chief attributes of the nanoscale refer to size ranges of the order of 1–100 nm, with the relevant nano-object defined as a material with one, two, or three external dimensions in the nanoscale [2]. Examples of such nano-objects include atom thick graphene sheets [3, 4], cylindrical carbon nanotubes [5, 6], and quantum dots [7]. Consequently, (1) the large surface area to volume ratio and the possibility of (2) the discretization/quantization of the energy levels, due to quantum confinement, are seen as two immediate consequences of the nanoscale. From the point of view of electrical charge based energy storage (as in batteries [8] and capacitors [9, 10]), it may be thought that while larger surface area/volume ratio may imply an easier access to charge storage (with the possibility of fast charging and discharging), quantization could imply the tuning and obtaining of a specific voltage. On the other hand, the reduced volume would also imply lower charge and energy capacity overall and it is unclear whether carrier confinement and energy quantization would be useful for energy delivery. Moreover, several practical issues such as durable and reliable contacts to the nanoscale objects that tap the charge and energy to a three-dimensional world and the possibility of contaminating influences from the ambient could be problematic. To truly understand the potential of the nanoscale objects and materials, it would then be relevant to further probe the attributes, and it is the purpose of this review to consider in detail the universal and fundamental material characteristic, i.e. the necessary presence of defects, guaranteed through entropic considerations. To this end, the review will briefly consider how the natural and induced defects on nanoscale materials, such as nanotubes and graphene, would be measured, monitored, and harnessed. The focus will be on nanocarbons due to their closeness to activated carbon (AC), which is of widespread use in the battery and capacitor technologies. Considering that nanostructures have been defined predominantly in terms of

*Corresponding author: Prabhakar R. Bandaru, Room 258, Engineering 2, Department of Mechanical Engineering, 9500 Gilman Drive, MC 0411, UC, San Diego, La Jolla, CA 92093-0411, USA, Phone: +(858) 534-5325, e-mail: pbandaru@ucsd.edu; and Program in Materials Science, Department of Mechanical Engineering, University of California, San Diego, La Jolla, CA 92093-0411, USA
Hidenori Yamada: Department of Electrical Engineering, University of California, San Diego, La Jolla, CA 92093-0411, USA
Rajaram Narayanan: Department of Nanoengineering, University of California, San Diego, La Jolla, CA 92093-0411, USA
Mark Hoefer: Program in Materials Science, Department of Mechanical Engineering, University of California, San Diego, La Jolla, CA 92093-0411, USA

their relatively large surface, such attributes seem to be relevant for probing large area devices, as these are relevant for electrochemical capacitors (ECs). Redox reactions, particular to battery-type architectures, will not be significantly considered here. The role of defects in modulating battery electrode characteristics, through interfacial reactions, has also been reviewed previously.

The charge capacity of a nanostructure is related to the electrical capacitance of the device and will be considered first, with reference to practical EC. The review will then briefly consider the possible types of defects on the two-dimensional (2D) surfaces of nanostructures.

2 The charge storage capacity and capacitance of a 2D layered material that constituted EC

A measure of the ability of a structured material to hold electrical charge, under an applied potential difference, has been rationalized in terms of an electrical capacitance. The partitioning of the overall capacitance (C) of a structure into various constituents (Figure 1) yields insights into the mechanisms underlying the charge storage as well as the electrical and electrochemical characteristics of the material and related devices. For example, a layered 2D material could possess both a classical space-charge capacitance (C_{sc}) due to a spatial variation of the potential, as well as a quantum capacitance (C_Q) due to the finite density of states (DOS). However, a single-atom layered 2D material [i.e. a single-layered graphene (SLG)] would not have an assigned C_{sc}, which is ascribed to the screening of the ambient charge into the inner layers *by* the outer layers (also Section 2.4). Consequently, the extent to which the classical and the quantum capacitances are manifested would be a measure of the descriptors of lower dimensional materials and devices. Additionally, it would be important for correlating the measured C with the modeled constituents, whether the individual capacitances add in series or in parallel. We now discuss a few manifestations of the capacitance of prototypical 2D materials, e.g. few layer graphene (FLG) and SLG.

2.1 Double layer capacitance

The placement of a 2D material (on an electrode, for measurement) into an ambient would be associated with a charge separation due to the respective differences in the electrochemical potential and yields a net capacitance,
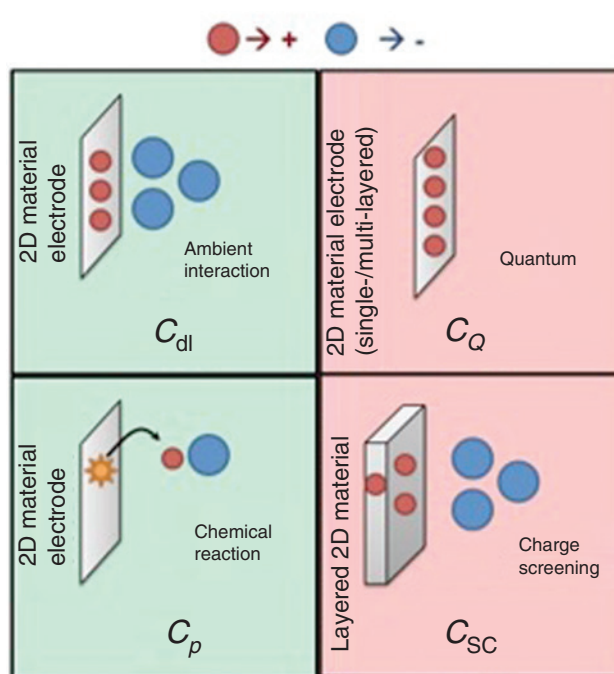
Figure 1: Schematic of a few manifestations of capacitance for a typical 2D material constituting an electrode (enabling electrical measurement). A positively charged 2D material-electrode is indicated, for example. The double-layer capacitance (C_{dl}) comprised of charges adjacent to the 2D material and due to electrostatic interactions with ambient, e.g. air, water, plasma, etc. The series addition of other capacitances also needs to be considered. These include a quantum capacitance (C_Q) – due to finite density of states, relevant to lower dimensions, a space-charge capacitance (C_{sc}) for layered 2D materials such as FLGs, due to the spread of the charge in the structure, and a chemical-/pseudo-capacitance (C_p) due to possible chemical (oxidation/reduction) reactions on the surface. A thorough understanding of such capacitances constitutes the goal of the proposed work and provides crucial insights into electrical properties of 2D materials and related devices and technologies.

from two contributions, i.e. a Helmholtz capacitance and a diffusion capacitance. For example, when the electrode is positive (negative), it would be surrounded by corresponding negative (positive) charge. The adjacent oppositely charged layers constitute a double-layer [11–14] capacitance. The resultant Helmholtz capacitance, C_H (per unit area), for the 2D material electrode, with charge stored in a layer of thickness (d) is given, in an elementary form, by the following:

$$C_H = \frac{\varepsilon}{d}. \tag{1}$$

In Eq. (1), $\varepsilon = \varepsilon_o \varepsilon_r$, with ε_o as the permittivity of free space and ε_r as the relative dielectric permittivity of the ambient. While d has conventionally been taken as the average separation distance between the positive and

negative charges, a more precise equivalence would be the Thomas-Fermi screening length, $\lambda_{T\text{-}F}(=\sqrt{2n\varepsilon e^2/E_F})$, which is related to the span over which the electrical carriers in the 2D material (of density, n, with e as elementary electron charge, and Fermi energy, E_F) exert their influence into the ambient [15].

2.2 Diffusion capacitance

Additionally, there would be a spread of the counteracting carriers/ions from the ambient away from the material, and the ratio of the resultant charge distribution and the potential variation yield the diffusion capacitance (C_D). The combination of C_D and C_H, in series, is generally considered as the net double-layer capacitance (C_{dl}). C_D is of the following form [16]:

$$C_D = \sqrt{\frac{2\varepsilon(ze)^2 I^o}{k_B T}} \cosh\left(\frac{ze\phi}{k_B T}\right). \qquad (2)$$

The above relation (with I^o as the ambient ion concentration and applied voltage/potential (ϕ) and with z as the magnitude of ion charge, e.g. +1 for H$^+$/Na$^+$ and –1 for OH$^-$/Cl$^-$, k_B is the Boltzmann constant and T is the temperature) is obtained through solving the Poisson-Boltzmann equation, with ambient carrier concentration varying as exp $(-e\tilde{\phi}k_B T)$. Concomitantly, Debye length (L_D) [16, 17] is considered to be a typical measure of the diffuse layer thickness constituting C_D and is given by the following:

$$L_D = \sqrt{\frac{\varepsilon k_B T}{2(ze)^2 I^o}}. \qquad (2a)$$

However, the cosh () term in Eq. (2) seems to indicate an increase of the capacitance without limit as the voltage (/ϕ) is increased. Such a conclusion is contrary to typical experimental observation where the saturation of the measured capacitance is observed with increasing voltage. Generally, at sufficiently large applied potentials, oppositely charged ions would indeed adhere strongly to the 2D material, with an average separation distance subject to limitations arising from ionic radius as well as the influence of the ambient (e.g. the solvation of the ions in aqueous systems). As I^o or ϕ is increased, at a given temperature, $C_D > C_H$, and the diffusion layer is increasingly irrelevant for the measured capacitance and can be discriminated. It may also be noted, for example, that at smaller ϕ, $C_{dl} \rightarrow C_D$; at ϕ (of the order of $3k_B T$), C_H and C_D are comparable; and at a larger ϕ (greater than 10 $k_B T$), $C_{dl} \rightarrow C_H$. There are yet issues in modeling

the precise magnitudes of C_D and C_H. It is unclear, for example, whether the bulk ambient dielectric permittivity [18] would be appropriate for distances close to the 2D material-ambient interface. The large electric field at the surface (due to the potential drop over a size scale of an ion) implies the necessity for considering orientational effects, e.g. of the water molecules from the ambient, in addition to enhanced polarization [19]. Consequently, ε_r may be considerably reduced, as much as an order of magnitude from the bulk value, e.g. in the case of ambient moisture/water, from ~78 to as low as 4.7 for H$^+$/OH$^-$ ion-2D material distances of the order of 0.1 nm (note that the radii of H$^+$ and OH$^-$ ions is ~0.09 nm and 0.155 nm, respectively). Such reduction in ε_r correspondingly reduces C_H and complicates understanding effects of ambient water on 2D materials [20]. Further experimental work is necessary to yield relevant insights into such issues.

2.3 Quantum capacitance

A characteristic particular to low dimensional materials, such as 2D graphene or one-dimensional (1D) nanotubes [5, 21], is the finite DOS. Consequently, there is a relatively larger increase (decrease) of Fermi energy (E_F) when electronic charge of magnitude $dQ (= e \cdot dn)$ is added (removed) due to an applied voltage change (dV) [22]. An effective quantum capacitance (C_Q) in series with the C_{dl} could be defined, considering DOS at the E_F, as follows:

$$C_Q = \frac{e \cdot dn}{(dE_F/e)} = e^2 \text{DOS}(E_F) \qquad (3)$$

A low C_Q generally indicates lack of available states that can be occupied, e.g. during charging and influences device characteristics. Broadly, a net applied voltage (ΔV) causes a differential change in E_F and would be partitioned between the 2D material (as ΔV_Q) and the surrounding ambient/environment (ΔV_E). While ΔV_Q would be associated with C_Q, ΔV_E is related to additional classical capacitances due to the internal and external environment of the 2D material. While C_{dl} is a manifestation of the latter, an aspect of internal charge re-distribution would be through a space-charge capacitance (C_{SC}) [23–25].

2.4 Space charge capacitance

An additional capacitance in series with C_{dl} and the C_Q, particular to layered 2D nanostructures such as FLGs, is C_{SC},

which arises due to the screening of the ambient charge into the inner layers by the outer layers, see Figure 2. With a carrier concentration (n) of the order of 5×10^{20}/cm^3, the screening distance would be ~0.34 nm – the thickness of a graphene sheet [3, 28]. The implication is that an atomic layer sheet would not completely screen the electric fields and a single-layer 2D material could not constitute a perfect electrode. The consequent internal charge diffusion and re-arrangement in the 2D material (with $\varepsilon = \varepsilon_o \varepsilon_r$ and with ε_r as the relative permittivity of the 2D material) implies a C_{sc} [29] as follows:

$$C_{SC} = \sqrt{\frac{2\varepsilon(ze)^2 n_{2D,1}}{k_B T}} \cosh\left(\frac{ze\phi}{k_B T}\right) = \frac{\varepsilon}{\lambda_{T\text{-}F}}. \tag{4}$$

While such a form seems similar to that of Eq. (2), $n_{2D,1}$ now refers to the carrier concentration in the first/outermost layer of the 2D material, immediately adjacent to the ambient, the charge of which is being screened into the other interior layers of the 2D material. Alternately, a single-layered 2D material (e.g. SLG) would not have a spread of charge into the interior and no C_{SC}. This would help in the further delineation of the constituents of the measured capacitance. Generally, the consideration of C_{SC} would also be very relevant for multiple-layered 2D materials (such as FLGs, MoS$_2$, WS$_2$, Mo$_2$P, etc.).
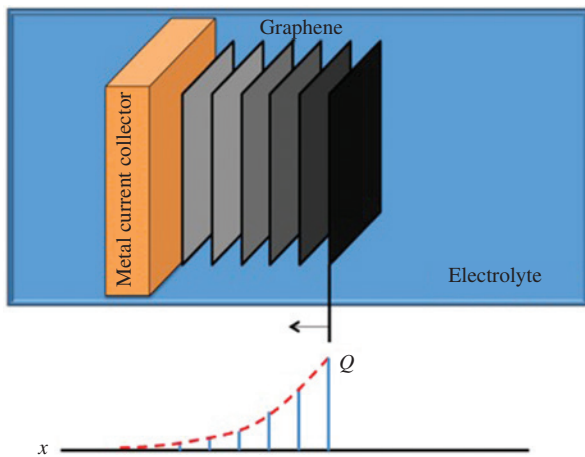
Figure 2: While the constituent charge in the individual layers of a 2D material may be considered discrete, the carrier concentration from the outermost layer into the current collector may be modeled through a continuous exponential decay. A concomitant length scale for the internal charge storage would be an equivalent Thomas-Fermi screening length [26] ($\lambda_{T\text{-}F}$). Additionally, immobile surface charges (due to defects) may also contribute to the space charge. (Figure adapted from Reference [27] and reproduced with permission from the American Chemical Society, 2015.)

2.5 Chemical capacitance

The net electrochemical potential (the Fermi energy: E_F) constituted the electrostatic potential (due to carrier density change at a point) and the chemical potential (due to carrier density being distributed over a representative volume element), yielding electrostatic capacitance and chemical capacitances, respectively. While the former has been previously discussed (e.g. through C_H, C_D, C_{SC}, etc.), the latter is manifested, for example, in a photo-electrochemical cell, as used for photo-electrochemical applications [30–32]. Consider, for example, a macroscopic capacitor constituting nanoscopic units arranged in a mesoscale architecture, e.g. TiO$_2$ nanoparticles on the electrode of a dye-sensitized solar cell (DSSC) [33]. The potential difference between the electrodes of the capacitor would be mostly concentrated on the nanoparticles and the interfaces, due to their large number. A chemical capacitance (C_{chem}) specific to such mesoscopic architecture may been defined [34] through the following:

$$C_{chem} = \frac{e.\partial N_i}{(\partial \mu_i / e)} = e^2 \frac{\partial N_i}{\partial \mu_i}. \tag{5}$$

The consideration of the nanostructured entities is done through the change of the number of charge states: N_i (for the ith nanoparticle/grain) corresponding to both the free electrons (of concentration, n_c) and localized/trapped electrons (of concentration, n_T for a given change in the chemical potential: μ_i). From the thermodynamic expression [35] $\mu_i = \mu_i^o + k_B T \ln (N_i)$, we may derive, e.g. $C_{chem} = e^2 N_i / k_B T$.

Thus far, the individual contributions to a measured capacitance (C_{meas}) have all been manifested through *series* contributions of the form (see Figure 3):

$$\frac{1}{C_{meas}} = \frac{1}{C_H} + \frac{1}{C_{diff}} + \frac{1}{C_{SC}} + \frac{1}{C_{chem}} + \frac{1}{C_Q} \tag{6}$$

It is obvious, from the relation above, that the lowest capacitance would dominate C_{meas}, e.g. through a low C_Q for 2D materials of the order of ~2 μF/cm^2 [36–39] due to the very low DOS. Alternately, a very high capacitance – of the order of 500 μF/cm^2 – is typical of C_H, from Eq. (1). Moreover, 2D material based nanostructures have been postulated to have a theoretical surface area per mass of the order of, e.g. ~2600 m^2/g for graphene [40, 41]. Consequently, the theoretical maximum possible capacitance density may be thought to be of the order of 13,000 F/g (from the product of 500 μF/cm^2 and 2600 m^2/g). However, the reported/measured capacitances are orders of magnitude lower [42], at ~100 F/g [43–47]. It
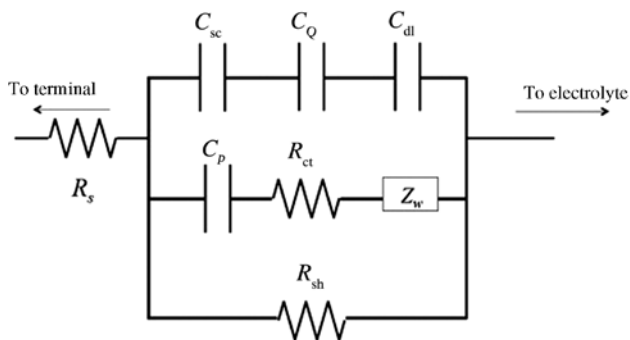
Figure 3: A possible impedance model consisting of additional resistance and capacitance contributions in 2D material that constituted nanostructured electrodes. In non-metallic materials, space charge capacitance – C_{sc} (see Section 2.3), quantum capacitance – C_Q (see Section 2.4), in addition to a Faradaic/surface area-dependent pseudocapacitance or chemical capacitance – C_p (see Section 2.5), as well as concomitant leakage/shunt resistances – R_{sh}, may be present.

can now be understood that low measured capacitances arise from the (a) series addition of various classical and quantum capacitances, as described through Eq. (6), as well as (b) incomplete/inadequate utilization of surface area [48].

Moreover, we specifically address the influence of the real surface area contributing to the charge storage. C_{meas} would be expected to be directly proportional to such an area. The utility of edge planes, which do not directly contribute to the projected area but which have been hypothesized as contributing to the charge density [49–52], could thus be verified.

3 The characteristics and topology of defects on 2D material surfaces and their influence in charge and energy storage

It is interesting to ponder why an SLG sheet would have a comparatively higher capacity or energy density [53–55], compared to bulk/bulk-like materials. Indeed, earlier works [13, 56] reported the C_{dl} value of a clean graphite surface as ~20 μF/cm^2, typical to any other thin film providing a benchmark for what may be experimentally observed. Moreover, the SLG sheet-substrate interaction, as manifested in phonon coupling [57, 58] or surface assisted coupling based synthesis [59], indicates the difficulty in precisely ascribing characteristics typical of a single independent sheet.

Additionally, multiple graphene sheets/FLGs, which may be considered to have a limiting case of bulk structures, have been shown to have relatively higher capacitance [60, 61]. Consideration of intermolecular forces between the atomic-scale sheets [62] may need to be considered for charge storage. A fundamental basis for adsorption-induced enhancement of the capacitance may arise from van der Waals forces induced through the π-orbitals. Indeed, the larger currents at a given voltage scan rate in FLG compared to the SLG samples may be accounted for through such considerations. Alternately, by examining the pore structure of ACs, the ratio of the pore wall thickness to the Debye length in the electrolyte would be relevant. Through comparison with a variety of ACs, it was deduced that enhanced capacitance, i.e. to a limit of up to ~80 F/g may be obtained through a decreasing ratio only up to a limit. Physically, this would correspond to an overlapping of the screening lengths. These results may then be extrapolated to a single graphene sheet, where the applied voltage/potential is not constant, and to realize the ability of graphene to function as a proper electrode, multiple layers, up to four, may be necessary [61]. Concomitantly, it may be necessary to understand the influence of termination of the graphenes or related 2D materials.

Useful nanoscale prototypes for understanding the influence of defects are, for example, the basal planes and the edge planes of graphite surfaces. It has been widely reported that the former are chemically inert, while the latter are considered to be sites of electrochemical reactivity [49–51, 63]. In the edge plane, for example, defects can induce different bond orderings and bond configurations. If bond reordering occurs without the addition of vacancies or other atoms, the armchair and zigzag configurations are formed. These configurations are relatively stable in graphene-based structures as they have the fewest dangling bonds, which represent centers of charge concentration. Specific techniques, involving structural characterization such as Raman spectroscopy and electrochemical techniques, have been recently shown to identify the armchair and zigzag configuration induced defects in FLG structures [27] (Figure 4).

The in-plane sp^2 bonding on each constituent graphene sheet of the graphite involves the pendant π – groups, which may be indirectly involved in charge transfer through weak bonding and adsorption processes [64]. The enhancement in the surface DOS due to the formation of localized states [65] may also be correlated with an increased capacitance. While passivation of the surface states, say through a C-H bond, may occur, it has been posited that the σ-bond would not interact with the π-orbitals and disrupt electronic
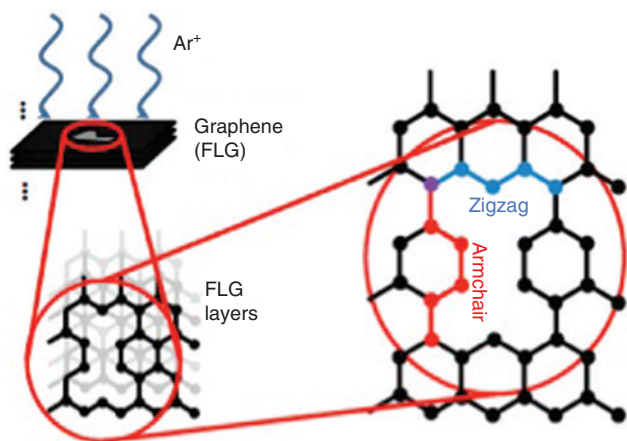
Figure 4: Identification of charged states in FLGs. Argon ion based plasma processing was used to purposefully create and then identify defects (such as dangling bond-rich edge plane defects of the armchair or zigzag varieties) and their contribution to capacitance and energy storage, in FLG structures. (Figure adapted from Reference [27] and reproduced with permission from the American Chemical Society, 2015.)

structure. Additional energy states may be introduced through curvature-induced modification of single/multiple graphene sheets, for example, in wrinkled 2D material sheets. The extent to which experimental results studies indicate the relative absence of electrochemical reactions on basal planes, compared to edge planes, is difficult to gauge *vis-à-vis* the inevitable presence of atomic scale/nanoscale defects. While an upper limit value of $k_{basal} = 10^{-9}$ cm s^{-1} was used for modeling the basal plane electrokinetics (with k_{edge} seven orders of magnitude larger at 0.02 cm s^{-1}), these numbers are yet estimates. It was interesting to note that in an alternate analysis comparing the reduction of quinone on basal planes and edge planes [51], the electron transfer rate (now expressed [66] in units of s^{-1}) of the rate constants of the latter was only two to three orders of magnitude larger.

It has also been observed, through scanning tunneling microscopy studies [67], that adsorption tracks the defect area (given that the proportion of the defect area to the total projected area has been estimated to be of the order of 0.01 to 0.1) only qualitatively but may be orders of magnitude higher than expected. There may also exist electrostatic interactions between the adsorbates and partial charges on the surface, which may extend over a larger area than a charged defect. Moreover, functional groups as well as the polarity of the surface [68] may enhance the sticking coefficient of adsorbates at the monolayer level. It has also been speculated that adsorption could occur concurrently with intercalation (as with anodes in battery systems) where the latter is more probable at the edge

planes. In summary, the electrochemical characteristics of nanostructured 2D material constituting electrodes still remain to be well understood, with reference to the role of defects and disorder. It then becomes necessary to model defective nanomaterials (e.g. constituting the electrodes in batteries) for realistic perspectives on energy storage capacity. Intrinsic defects generally result from structural changes in the lattice without the introduction of impurity atoms, while extrinsic defects may involve impurity atoms. In addition to structural effects, defects may also produce unique changes in the electronic properties. Moreover, impurity electronegativity and atomic or ionic size can affect the lattice interactions. Such defects in any given structure, or nanomaterial, are inevitable in that the addition of any impurity in any amount would necessarily increase the entropy: S [69]. It can be derived [70] that the concentration of point defects (n_d), relative to the total number of atoms in the sites in the structure (N), is given

by $\dfrac{n_d}{N - n_d} = \exp\left(-\dfrac{(E_F - TS)}{k_B T}\right)$, also considering the energy

of formation (E_f). In the simplest case, a vacancy (when the lattice is missing an atom) may form. Additional lower dimensional defects such as vacancy clusters, interstitial adatoms, or lattice impurities are widely manifested, e.g. in nanocarbons. Such defects induce changes in the bonding structure in addition to inducing local bond strain. The energy of formation for single vacancies, $E_{f,SV}$, is ~5–9 eV. The variation in the formation energy of ~4 eV could be a function of the sample size, i.e. as in the effective size of the 2D material [71]. It should also be noted that the computation of the formation energies of the defects is fraught with issues of correctly estimating the ground state energy [71, 72]. In the case of graphenes, if a single vacancy is created, carbon atoms surrounding the vacancy are at a relatively higher energy state, as they are not fully coordinated and have dangling bonds. Such higher energy carbon atoms may undergo Jahn-Teller distortions (geometrical distortion to reach a lower energy state [73]) to minimize the local energy, forming a pentagon and a nonagon with one dangling bond remaining.

Vacancies can be mobile if enough energy is provided to overcome a geometry-dependent migration barrier $E_{mb,SV}$ of ~0.5–2 eV [74]. Subsequently, if two vacancies join, a double vacancy is formed with an energy of formation $E_{f,DV}$ of ~4–5.5 eV [74]. In a double vacancy, there are no dangling bonds as two pentagons and a heptagon form, which are relatively immobile with a migration barrier $E_{mb,DV}$ of ~5 eV [74]. Consequently, intrinsic or extrinsic defects may be defined at any location where the periodic arrangement is perturbed.

Extrinsic defects and associated charges may also be purposefully induced in 2D material structures through adatoms/particles, vacancies, substitutional impurities, etc. The methods for their introduction may, for example, be through (1) irradiation with electrons or ions [75–77] and (2) chemical treatments, e.g. through oxidation induced wet chemistry. Consequently, the electronegativity and ionization potential of an adatom can determine, to a first order, whether the adatom has a propensity for drawing electrons away or donating electrons to the surrounding bonds. The injection or withdrawal of electrons into π-bonds may be considered a form of doping. As π-bond electrons are extensively delocalized in graphene, π- and $\pi^\star$-orbitals may constitute the valence and conduction bands, respectively.

When electron-deficient moieties are added to graphitic structures either through bonding, adatom introduction, or substitutional impurity addition, energy levels in proximity to the regular bands may be created. For example, when B or N (of approximately the same size as carbon) with one less/more electron than carbon is added to graphitic structure, the carbon atoms are replaced (Figure 5). The charge density shifts creating a partial positive/negative charge on the surrounding carbons and

new defect energy levels are created near the valence/conduction band.

Instances of electron withdrawal and donation with respect to the graphitic structures may then occur when B and N are added substitutionally. Such downward or upward variations in the Fermi energy modulate the voltage and the consequent current in charge transfer from a given nanostructured electrode to the electrolyte. Changes in the net electrochemical potential would then dictate the reactivity of the constituent bonds and can increase electrocatalytic activity or charge transfer from the electrode.

Extrinsic point defects may also arise from the addition of adatoms on the surface of the nanostructures. If the adatoms are smaller than the inter-graphitic spacing of ~0.35 nm, they can reside interstitially [79] facilitating the formation of two new covalent bonds (with a binding energy associated with the bond formation of ~2 eV [80]) to the surrounding carbons and an sp^3 character. In the case of carbon adatoms, the migration barrier is 0.4 eV, implying high adatom mobility along the graphitic surfaces. For non-carbon adsorbed atoms or adsorbed particles, the electronic interaction energies would vary with the state and size of the adatom and its size (e.g. physisorption through van der Waals forces or chemisorption through bonding to the surface). Given a typical metal reduction potential of ~2.5 V (with respect to the standard hydrogen electrode), adatom bonding to defects would occur if the defect energies are larger.

When foreign atoms add as substitutional impurities into the graphitic lattice, say, for the purpose of doping, they may also be considered to be point defects. Thermodynamically stable substitutional impurities tend to be similar in atomic size and have a close number of valence electrons, e.g. boron or nitrogen for carbon based 2D materials. However, when coupled with vacancies, a broader variety of substitutions can occur. Transition metals may also form strong covalent bonds (with bonding energies ~2–8 eV) at vacancy sites by coordinating with dangling bonds [71, 81, 82]. Typically, the E_f values are greater than 1 eV and may be as large as 14 eV (for an adsorbed atom-single vacancy pair [71]). Many such defects are evident as a function of specific synthesis conditions and contribute to variable electrochemical characteristics. Generally, lower dimensional defects, e.g. point/zero-dimensional defects, such as vacancies, interstitial, or substitutional defects, are more favorable compared to 1D or 2D defects such as dislocations or boundaries, which impose a formation energy (E_f) penalty.
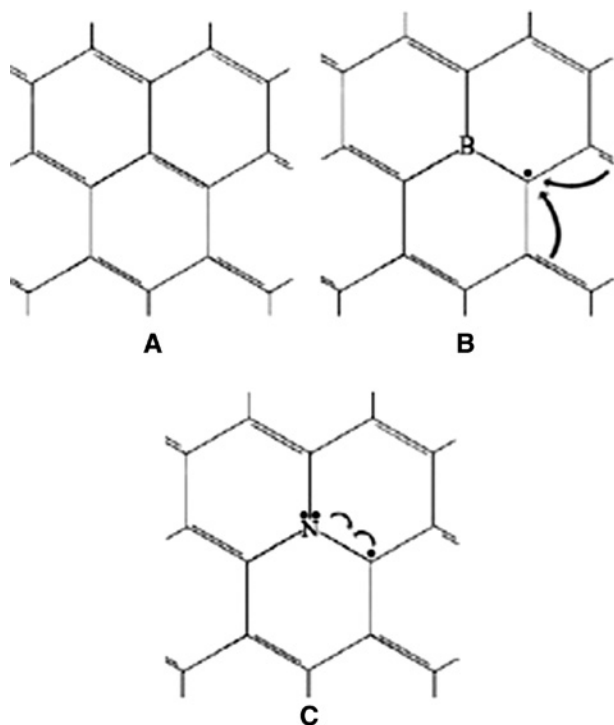
Figure 5: Illustrations of delocalized π-bonding in (A) pristine, (B) boron (B-) doped, and (C) nitrogen (N-) doped graphitic structures. (Adapted from Reference [78].)

4 Issues in harnessing the charge in nanostructures for technological application

Consequent to the practical necessity of considering and modeling defects (in various dimensionality) to charge and capacitance modulation, there yet remain several practical issues in the suitable harness of energy and utility of nanostructured electrodes for energy storage. These encompass the proper accounting of the electrode area, whether all the parts of the electrode are even in contact with the electrolyte, etc. Such issues will be discussed next.

4.1 The extent of the surface area in nanostructured materials and electrodes

A major issue in quantifying and correlating the capacitance to theoretical estimates is the accurate knowledge of the effective area (A_{eff}) of charge transfer, such that the relevant unit capacitance (i.e. capacitance per unit area: C_{Area}) can be rigorously determined. While conventionally, the projected area of a 2D material that constituted a substrate is considered, more accurate and precise determination of the area is generally warranted to consider the (a) different charge storage capacities of the constituent moieties (e.g. to determine the extent to which Mo and S in MoS_2 store charge), (b) multi-layered 2D materials and constituent edges, (c) defects and adsorbed moieties, which may/may not participate in charge transfer, etc. Such characterization is crucial in that the capacitance density (capacitance per unit mass: C_{Mass}) is often estimated by multiplying C_{Area} by the areal density (in units of m^2/g) – determined through gas adsorption analysis. It is then seen that there is much disparity and consequent confusion in reported values of C_{Mass} in literature, as (i) gas adsorption analysis overestimates the available area, gas molecules have greater access to nanostructure porosity compared to electrolyte molecules/ions, and (ii) the projected (and not the actual) area is often used for evaluating C_{Area}. It is then required to develop accurate metrics and methodologies for reporting C_{Area} as well as C_{Mass}, with an aim to measure and crosscheck the real A_{eff} of 2D material structured electrodes. The area may be estimated, e.g. through both the experimentally measured maximum/net current considering the major possible electrochemical processes [16, 17], as well as through a complementary methodology, employing integrated currents (i.e. charge) to verify the A_{eff} value obtained above. Here, as an initial

voltage step, the total charge passed to the solution (Q^{tot}) could be defined through the sum of the charges relevant to (i) diffusion related processes (Q_{diff}), (ii) adsorbed species (Q_{ads}), and (iii) double layer (Q_{dl}) [17]. As charge transfer to the adsorbed species (Q_{ads}) and the double layer (Q_{dl}) occur on a relatively shorter time scale than charge transfer arising from diffusion processes, Q_{diff} can be isolated from the effects related to $Q_{dl} + Q_{ads}$ allowing for the estimation of A_{eff}.

The use of nanostructured materials in electrodes would also pose problems related to the extent to which the electrolyte is fully in contact with the constituent area, for charge transfer interactions to occur. Such issues may be discussed with respect as to whether the electrolyte wets the electrode and is a function of the respective surface energies as well as physical characteristics such as the roughness of the electrode, etc. Classical monographs [83] describe such interactions fundamentally by considering a wetting/spreading parameter (Sp) of the form $Sp = \gamma_{s-a} - (\gamma_{s-e} + \gamma_{e-a})$, where the subscripts refer to the relative surface energies of the solid electrode-air, solid electrode-electrolyte, and the electrolyte-air interfaces, respectively. Generally, when $Sp > 0$, the electrode prefers to be wetted by the electrolyte and good contact would be ensured. It was postulated that idealized interactions between the individual constituents could make it possible to relate Sp to the individual polarizabilities (surface energies being related to the square of the polarizability [62]). Consequently, an electrolyte would spread on/wet completely the electrode, if it was less polarizable than the solid electrode. Concomitantly, it can be adduced that enhancing the polarization of the electrode, e.g. as in metallic materials or through the edge planes in graphite, or defects would favor greater contact between the electrode and electrolyte. A prototypical example of roughness at the nano-, meso-, and macroscale is practically manifested through porous carbon/AC-based electrodes in ECs.

The relative dielectric constants (ε) of the electrolyte (ε_e) and the material constituting the electrode (ε_{el}) should also be considered. For aqueous electrolytes, one should also consider the relative hydrophobic and hydrophilic character of the surfaces, e.g. the latter may be enhanced through the presence of polar moieties and charged defect states. On the other hand, hydrophobic surfaces may be stochastically wetted/de-wetted by water for pore sizes of the order of 0.7–0.8 nm [84]. A ratio of the actual area to the apparent projected area has been used to describe the wetting characteristics and may also be extrapolated to estimate the enhanced charge density of a rough surface. Alternatively, another quantitative methodology involves

the use of the current-potential curves obtained from surface adsorption based pseudocapacitance [85], e.g. the ratio of the theoretical maximum capacitance to the measured capacitance would yield a measure of the roughness to within ±40–50% [85]. A roughness factor has also been used in estimating the capacitance of nanostructured electrodes, e.g. in dye-sensitized solar cells (DSSCs). Here it was assumed that the Helmholtz capacitance (C_H) would be similar for any two surfaces and the roughness factor is used to multiply the capacitance of a smooth surface to obtain the capacitance of the rough surface [86]. Additionally, corrugations and the local curvature of the surface could simulate pore-like behavior and influence the observed characteristics. While the complexity of the problem and the general irreproducibility across samples have resulted in ignoring such issues, roughness yet remains a very important issue in understanding the effective area of a nanostructured material constituting electrode as well as for correlating the theoretical predictions to experiments.

4.2 Issues due to energy discretization in nanostructures

A major issue in harnessing charge from nanostructures is ensuring compatibility of the associated energy scales between the nanoscale – where the charge is stored – and the macroscale – to which the charge is transferred. If there is an incompatibility, e.g. considering the difference in the DOS, where a discrete distribution is obtained for the nanoscale and a continuous distribution for the macroscale, an energy barrier [29] would exist with the technological implication of different times for charging and discharging the energy storage device. Only in those cases where the equivalent width of the barrier region is sufficiently small may carriers tunnel through yielding a quasi-Ohmic behavior and equivalent times for charge/discharge. Such behavior has been observed, and typically for nanostructure lengths <1 μm, electrical transport does seem to be limited by the Schottky barriers at the metal-semiconductor interface. However, for greater lengths and in lower dimensionality, there would be a stronger influence of the defects/impurities (as outlined in Section 3), which may induce a strong resonant backscattering and reduce carrier mobility [87]. Such defects in nanomaterials would also contribute significantly to a combined capacitive and battery-like behavior, as has been found in large specific area aerogels [88] and carbon nanotubes [40, 89, 90]. An example of the practical necessity for the consideration of quantum effects is the manifestation of an additional quantum capacitance (C_Q) – in series with the electrostatic capacitance, which is directly proportional to the DOS of the pertinent nanostructures – as discussed in detail in Section 2.3. The series addition implies that the C_Q needs to be larger than the nominal electrostatic contribution for its neglect, which would typically not be possible, as nanostructures intrinsically possess a smaller number of states with a smaller C_Q.

In addition to the scientific issues related to the adequate utilization and parameterization of the surface area as well as the finite DOS due to nanostructuring discussed in the previous two sections, there are a host of more practical problems related to the use of nanostructured electrodes. While a comprehensive discussion of such problems, which may include low packing densities (which contributes to low volumetric energy density in distinction to gravimetric energy density), undesirable parasitic reactions with the electrolyte (stemming from the large surface area to volume ratio of the constituents of the electrodes), and high manufacturing costs are outside the scope of the present review, the reader is encouraged to consult a paper [91] related to charge transfer and storage in nanostructures, which considers such aspects in more detail. For example, while 1D nanostructures have a higher electronic DOS at lower energies compared to bulk materials, the net amount of electrons could be smaller. As macroscopic properties such as electrical conductivity would be proportional to the net amount, nanostructured electrodes could have inferior electrical characteristics. Alternately, if 1D nanostructures could be packed tightly so as to occupy the same volume as the bulk, there would then be the possibility of higher electrical conduction efficiency (due to lower scattering in 1D channels), but such aspects are difficult to implement in a viable manufacturing process. The disadvantages accrued from non-close packing would be manifested in the accumulation of undesirable ambient impurities. Indeed, such extrinsic aspects may circumscribe the extent of possible usage of the nanomaterials even more than the possible advantages that may accrue from the lower dimensionality.

5 Conclusions

A major imperative for continuing research in charge storage is the exploration of new storage mechanisms as well as alternate materials systems where such mechanisms could be harnessed. Considering that carbon-based materials are ubiquitous, i.e. as graphite-based anodes in battery systems, or as AC electrodes in ECs, much of the

review has focused on morphologies and characteristics (e.g. edge and basal planes) particular to such materials. However, the increasing utilization of alternative 2D materials and associated van der Waals solids [92] on a larger scale makes many of the discussed issues, i.e. consideration of the various components of the capacitance (as in Section 2), the role of the inevitably present defect states in modulating charge and charge storage (as in Section 3), and the harness of the nanostructural attributes, with respect to the inducement of roughness and wetting of the electrodes, as well as possible quantum considerations (as in Section 4), relevant to alternate 2D materials as well. Whether 2D materials can definitely be proven to have advantages over conventional and presently used systems and be used for enhanced and optimal energy transduction and storage hinges on a successful resolution of such issues.

References

[1] Nelson DJ, Strano M. Richard Smalley: saving the world with nanotechnology. *Nat. Nanotechnol.* 2006, 1, 96–97.

[2] ISO/TS 27687:2008 – Nanotechnologies – terminology and definitions for nano-objects – nanoparticle, nanofibre and nanoplate. Available at: http://www.iso.org/iso/catalogue_detail?csnumber=44278. Accessed 16 August, 2014.

[3] Kastnelson MI. *Graphene: Carbon in Two Dimensions*. Cambridge University Press: Cambridge, UK, 2012.

[4] Novoselov KS, Jiang Z, Zhang Y, Morozov SV, Stormer HL, Zeitler U, Maan JC, Boebinger GS, Kim P, Geim AK. Room temperature quantum hall effect in graphene. *Science.* 2007, 315, 1379.

[5] Bandaru PR. Electrical properties and applications of carbon nanotube structures. *J. Nanosci. Nanotechnol.* 2007, 7, 1239–1267.

[6] De Volder MFL, Tawfick SH, Baughman RH, Hart AJ. Carbon nanotubes: present and future commercial applications. *Science* 2013, 339, 535–539.

[7] Jacak L, Hawrylak P, Wojs A. *Quantum Dots*. Springer: New York, 1998.

[8] Linden D, Reddy TB. *Linden's handbook of batteries*. McGraw Hill: New York, NY, 2010.

[9] Burke AF. Electrochemical capacitors. In *Linden's Handbook of Batteries*. Reddy TB, Linden D, Eds. McGraw Hill: New York, NY, 2011.

[10] Meller M, Menzel J, Fic K, Gastol D, Frackowiak E. Electrochemical capacitors as attractive power sources. *Solid State Ionics* 2014, 265, 61–67.

[11] Grahame DC. The electrical double layer and the theory of electrocapillarity. *Chem. Rev.* 1947, 41, 441–501.

[12] Delahay P. *Double Layer and Electrode Kinetics*. Interscience: New York, NY, 1965.

[13] Shi H. Activated carbons and double layer capacitance. *Electrochim. Acta* 1996, 41, 1633.

[14] Barbieri O, Kötz R. Capacitance limits of high surface area activated carbons for double layer capacitors. *Carbon* 2005, 43, 1303–1310.

[15] Lewerenz HJ. On the structure of the Helmholtz layer and its implications on electrode kinetics. *ECS Trans* 2013, 50, 3–20.

[16] Bard AJ, Faulkner LR. *Electrochemical Methods: Fundamentals and Applications*. 2nd ed. John Wiley: New York, 2001.

[17] Rieger PH. *Electrochemistry*. 2nd ed. Chapman and Hall: New York, 1994.

[18] Conway BE, Bockris JO, Ammar IA. The dielectric constant of the solution in the diffuse and Helmholtz double layers at a charged interface in aqueous solution. *Trans. Faraday Soc.* 1951, 47, 756.

[19] Webb TJ. The free energy of hydration of ions and the electrostriction of the solvent. *J. Am. Chem. Soc.* 1926, 48, 2589–2603.

[20] Li Q, Song J, Besenbacher F, Dong M. Two-dimensional material confined water. *Acc. Chem. Res.* 2015, 48, 119–127.

[21] Bandaru PR, Pichanusakorn P. An outline of the synthesis and properties of silicon nanowires. *Semicond. Sci. Tech*. 2010, 25, 024003.

[22] Datta S. *Quantum Transport: Atom to Transistor*. Cambridge University Press: New York, 2005.

[23] Sze SM. *Semiconductor Devices: Physics and Technology*. 2nd ed. John Wiley & Sons, Inc.: Singapore, 2003.

[24] Muller RS, Kamins TI. *Device Electronics for Integrated Circuits*. 2nd ed. John Wiley: New York, 1986.

[25] Gerischer H. Principles of electrochemistry. In *The CRC Handbook of Solid State Electrochemistry*. Gellings PJ, Bouwmeester HJM, Eds. CRC Press: Boca Raton, FL, 1997.

[26] Ashcroft NW, Mermin ND. *Solid State Physics*. Saunders College: Orlando, FL, 1976.

[27] Narayanan R, Yamada H, Karakaya M, Podila R, Rao AM, Bandaru PR. Modulation of the electrostatic and quantum capacitances of few layered graphenes through plasma processing. *Nano Lett.* 2015, 15, 3067–3072.

[28] Kuroda MA, Tersoff J, Martyna GJ. Nonlinear screening in multilayer graphene systems. *Phys. Rev. Lett.* 2011, 106, 116804.

[29] Sze SM, Ng KK. *Physics of Semiconductor Devices*. Wiley-Interscience: Hoboken, NJ, 2006.

[30] Grätzel M. Photoelectrochemical cells. *Nature* 2001, 414, 338–344.

[31] Döscher H, Geisz JF, Deutsch TG, Turner JA. Sunlight absorption in water – efficiency and design implications for photoelectrochemical devices. *Energy Environ. Sci.* 2014, 7, 2951.

[32] Peter L, Ponomarev E, Franco G, Shaw N. Aspects of the photoelectrochemistry of nanocrystalline systems. *Electrochim. Acta* 1999, 45, 549–560.

[33] O'Regan B, Grätzel M. A low-cost, high-efficiency solar cell based on dye-sensitized colloidal TiO2 films. *Nature* 1991, 353, 737–740.

[34] Bisquert J. Chemical capacitance of nanostructured semiconductors: its origin and significance for nanocomposite solar cells. *Phys. Chem. Chem. Phys.* 2003, 5, 5360.

[35] Ibach H, Luth H. *Solid-State Physics: An Introduction to Theory and Experiment*. Springer-Verlag: Berlin, 1991.

[36] Xia J, Chen F, Li J, Tao N. Measurement of the quantum capacitance of graphene. *Nat. Nanotechnol.* 2009, 4, 505–509.

[37] Cline KK, McDermott MT, McCreery RL. Anomalously slow electron transfer at ordered graphite electrodes: influence of electronic factors and reactive sites. *J. Phys. Chem.* 1994, 98, 5314–5319.

[38] Chen P, Fryling MA, Mccreery RL. Electron transfer kinetics at modified carbon electrode surfaces: the role of specific surface sites. *Anal. Chem.* 1995, 67, 3115–3122.

[39] Rice RJ, McCreery RL. Quantitative relationship between electron transfer rate and surface microstructure of laser-modified graphite electrodes. *Anal. Chem.* 1989, 61, 1637–1641.

[40] Hoefer M, Bandaru PR. Electrochemical characteristics of closely spaced defect tuned carbon nanotube arrays. *J. Electrochem. Soc.* 2013, 160, H360–H367.

[41] Peigney A, Laurent C, Flahaut E, Basca RR, Rousset A. Specific surface area of carbon nanotubes and bundles of carbon nanotubes. *Carbon* 2001, 39, 507–514.

[42] Simon P, Gogotsi Y. Materials for electrochemical capacitors. *Nat. Mater.* 2008, 7, 845–854.

[43] Huggins R. Supercapacitors and electrochemical pulse sources. *Solid State Ionics* 2000, 134, 179–195.

[44] Miller JR, Burke AF. Electrochemical capacitors: challenges and opportunities for real-world applications. *Electrochem. Soc. Interface* 2008, 17, 53–57.

[45] Burke A. Ultracapacitors: why, how, and where is the technology. *J. Power Sources.* 2000, 91, 37–50.

[46] Miller JM. *Ultracapacitor applications*. The Institution of Engineering and Technology: Herts, UK, 2011.

[47] Miller JR. Valuing reversible energy storage. *Science.* 2012, 335, 1312–1313.

[48] Radovic LR, Gogotsi Y. Surface chemical and electrochemical properties of carbons. In *Carbons for Electrochemical Energy Storage and Conversion Systems*. Beguin F, Frackowiak E, Eds, CRC Press: New York, 2010.

[49] Ji X, Banks C, Crossley A, Compton R. Oxygenated edge plane sites slow the electron transfer of the ferro-/ferricyanide redox couple at graphite electrodes. *J. Phys. Chem.* 2006, 7, 1337–1344.

[50] Banks CE, Davies TJ, Wildgoose GG, Compton RG. Electrocatalysis at graphite and carbon nanotube modified electrodes: edge-plane sites and tube ends are the reactive sites. *Chem. Commun.* 2005, 7, 829–841.

[51] Neumann CCM, Batchelor-McAuley C, Downing C, Compton RG. Anthraquinone monosulfonate adsorbed on graphite shows two very different rates of electron transfer: surface heterogeneity due to basal and edge plane sites. *Chem. A Eur. J.* 2011, 17, 7320–7326.

[52] Wiggins-Camacho JD, Stevenson KJ. Effect of nitrogen concentration on capacitance, density of states, electronic conductivity, and morphology of N-doped carbon nanotube electrodes. *J. Phys. Chem. C* 2009, 113, 19082–19090.

[53] Stoller MD, Park S, Zhu Y, An J, Ruoff RS. Graphene-based ultracapacitors. *Nano Lett.* 2008, 8, 3498–3502.

[54] Zhu Y, Murali S, Stoller MD, Ganesh KJ, Cai W, Ferreira PJ, Pirkle A, Wallace RM, Cychosz KA, Thommes M, Su D, Stach EA, Ruoff RS. Carbon-based supercapacitors produced by activation of graphene. *Science.* 2011, 332, 1537–1541.

[55] Ji H, Zhao X, Qiao Z, Jung J, Zhu Y, Lu Y, Zhang LL, MacDonald AH, Ruoff RS. Capacitance of carbon-based electrical double-layer capacitors. *Nat. Commun.* 2014, 5, 3317.

[56] Kinoshita K. *Carbon: Electrochemical and Physicochemical Properties*. John Wiley & Sons, Inc.: New York, NY, 1988.

[57] Pisana S, Lazzeri M, Casiraghi C, Novoselov KS, Geim AK, Ferrari AC, Mauri F. Breakdown of the adiabatic born-Oppenheimer approximation in graphene. *Nat. Mater.* 2007, 6, 198–201.

[58] Seol JH, Jo I, Moore AL, Lindsay L, Aitken ZH, Pettes MT, Li X, Yao Z, Huang R, Broido DA, Mingo N, Ruoff RS, Shi L. Two-dimensional phonon transport in supported graphene. *Science.* 2010, 328, 213–216.

[59] Cai J, Ruffieux P, Jaafar R, Bieri M, Braun T, Blankenburg S, Muoth M, Seitsonen AP, Saleh M, Feng X, Müllen K, Fasel R. Atomically precise bottom-up fabrication of graphene nanoribbons. *Nature.* 2010, 466, 470–473.

[60] Uesugi E, Goto H, Eguchi R, Fujiwara A, Kubozono Y. Electric double-layer capacitance between an ionic liquid and few-layer graphene. *Sci. Rep.* 2013, 3, 1595.

[61] Wood BC, Ogitsu T, Otani M, Biener J. First-principles-inspired design strategies for graphene-based supercapacitor electrodes. *J. Phys. Chem. C* 2014, 118, 4–15.

[62] Israelachvili JN. *Intermolecular and Surface Forces*, 3rd ed, Academic Press: San Diego, 2011.

[63] Randin J-P, Yeager E. Differential capacitance study on the edge orientation of pyrolytic graphite and glassy carbon electrodes. *J. Electroanal. Chem.* 1975, 58, 313–321.

[64] Li Q, Batchelor-McAuley C, Compton RG. Electrochemical oxidation of guanine: electrode reaction mechanism and tailoring carbon electrode surfaces to switch between adsorptive and diffusional responses. *J. Phys. Chem. B* 2010, 114, 7423–7428.

[65] Kobayashi K. Electronic structure of a stepped graphite surface. *Phys. Rev. B* 1993, 48, 1757–1760.

[66] Lewis NS. An analysis of charge transfer rate constants for semiconductor/liquid interfaces. *Annu. Rev. Phys. Chem.* 1991, 42, 543–580.

[67] McDermott MT, McCreery RL. Scanning tunneling microscopy of ordered graphite and glassy carbon surfaces: electronic control of quinone adsorption. *Langmuir.* 1994, 10, 4307–4314.

[68] Kwon S, Vidic R, Borguet E. The effect of surface chemical functional groups on the adsorption and desorption of a polar molecule, acetone, from a model carbonaceous surface, graphite. *Surf. Sci.* 2003, 522, 17–26.

[69] Porter DA, Easterling KE. *Phase Transformations in Metals and Alloys*. Nelson Thornes: Cheltenham, UK, 1992.

[70] Kelly A, Groves GW. *Crystallography and Crystal Defects*. TechBooks: Herndon, VA, 1970.

[71] Banhart F, Kotakoski J, Krasheninnikov AV. Structural defects in graphene. *ACS Nano.* 2011, 5, 26–41.

[72] Li L, Reich S, Robertson J. Defect energies of graphite: density-functional calculations. *Phys. Rev. B* 2005, 72, 184109.

[73] Hoffmann R. *Solids and Surfaces, A Chemist's View of Bonding in Extended Structures*. VCH Publishers: New York, 1988.

[74] Krasheninnikov AV, Lehtinen PO, Foster AS, Nieminen RM. Bending the rules: contrasting vacancy energetics and migration in graphite and carbon nanotubes. *Chem. Phys. Lett.* 2006, 418, 132–136.

[75] Krasheninnikov AV, Nordlund K, Sirvio M, Salonen E, Keinonen J. Formation of ion-irradiation induced atomic scale defects on walls of carbon nanotubes. *Phys. Rev. B Condens. Matter.* 2001, 63, 245405.

[76] Terrones M, Banhart F, Grobert N, Charlier J-C, Terrones H, Ajayan PM. Molecular junctions by joining single-walled carbon nanotubes. *Phys. Rev. Lett.* 2002, 89, 75501–75505.

[77] Nichols J, Deck CP, Saito H, Bandaru PR. Artificial introduction of defects into vertically aligned multiwalled carbon nanotube ensembles: application to electrochemical sensors. *J. Appl. Phys.* 2007, 102, 64306.

[78] Hoefer MA. *Electrochemical Implications of Defects in Carbon Nanotubes*. University of California: San Diego, 2012.

[79] Kiang C-H, Endo M, Ajayan PM, Dresselhaus G, Dresselhaus MS. Size effects in carbon nanotubes. *Phys. Rev. Lett.* 1998, 81, 1869–1872.

[80] Lehtinen P, Foster A, Ayuela A, Krasheninnikov A, Nordlund K, Nieminen R. Magnetic properties and diffusion of adatoms on a graphene sheet. *Phys. Rev. Lett.* 2003, 91, 017202.

[81] Yazyev OV, Pasquarello A. Metal adatoms on graphene and hexagonal boron nitride: towards rational design of self-assembly templates. *Phys. Rev. B* 2010, 82, 045407.

[82] Krasheninnikov A, Lehtinen P, Foster A, Pyykkö P, Nieminen R. Embedding transition-metal atoms in graphene: structure, bonding, and magnetism. *Phys. Rev. Lett.* 2009, 102, 126807.

[83] de Gennes P-G, Brochard-Wyart F, Quere D. *Capillarity and Wetting Phenomena: Drops, Bubbles, Pearls, Waves*. Springer: New York, NY, 2002.

[84] Dzubiella J, Hansen J-P. Electric-field-controlled water and ion permeation of a hydrophobic nanopore. *J. Chem. Phys.* 2005, 122, 234706.

[85] Conway BE, Gileadi E, Dzieciuch M. Calculation and analysis of adsorption pseudo-capacitance and surface coverage from E.m.f. decay and polarization curves: applications to a decarboxylation reaction. *Electrochim. Acta*. 1963, 8, 143–161.

[86] Schlichthörl G, Huang SY, Sprague J, Frank AJ. Band edge movement and recombination kinetics in dye-sensitized nanocrystalline TiO_2 solar cells:a study by intensity modulated photovoltage spectroscopy. *J. Phys. Chem. B*. 1997, 101, 8141–8155.

[87] Fernandez-Serra M-V, Adessi C, Blasé X. Conductance, surface traps, and passivation in doped silicon nanowires. *Nanoletters* 2006, 6, 2674–2678.

[88] Dong W, Sakamoto JS, Dunn B. Electrochemical properties of vanadium oxide aerogels. *Sci. Technol. Adv. Mater.* 2003, 4, 3–11.

[89] Nichols JA, Saito H, Deck C, Bandaru PR. Artificial introduction of defects into vertically aligned multiwall carbon nanotube ensembles: application to electrochemical sensors. *J. Appl. Phys.* 2007, 102, 64306.

[90] Hoefer MA, Bandaru PR. Defect engineering of the electrochemical characteristics of carbon nanotube varieties. *J. Appl. Phys.* 2010, 108, 034308.

[91] Bandaru PR, Yamada H, Narayanan R, Hoefer M. Charge transfer and storage in nanostructures. *Mater. Sci. Eng. R Reports*. 2015, 96, 1–69.

[92] Geim AK, Grigorieva IV. Van Der Waals heterostructures. *Nature* 2013, 499, 419–425.

Bionotes

Prabhakar R. Bandaru
Room 258, Engineering 2, Department of Mechanical Engineering, 9500 Gilman Drive, MC 0411, UC, San Diego, La Jolla, CA 92093-0411, USA, Phone: +(858) 534-5325; and Program in Materials Science, Department of Mechanical Engineering, University of California, San Diego, La Jolla, CA 92093-0411, USA,
pbandaru@ucsd.edu

Prabhakar R. Bandaru is a Professor of Materials Science in the Mechanical Engineering Department at the University of California San Diego (UCSD). He has worked extensively in energy storage systems, including electrochemical capacitors (ECs) in terms of the fundamental materials physics and chemistry. He also pioneered the use of novel one-dimensional (e.g. nanotube and nanowire) and two-dimensional (e.g. graphene) nanostructures for new modalities in electrochemical storage and electronics.

Hidenori Yamada
Department of Electrical Engineering, University of California, San Diego, La Jolla, CA 92093-0411, USA

Hidenori Yamada is a graduate student in the Electrical Engineering Department at UCSD. He considered the limitations imposed by the electronic density of states in limiting the maximum current that could be obtained in electrochemical devices and contributed extensively on relevant quantum mechanical interpretations.

Rajaram Narayanan
Department of Nanoengineering, University of California, San Diego, La Jolla, CA 92093-0411, USA

Rajaram Narayanan is a graduate student in the Nanoengineering department at UCSD and avidly pursues electrochemical analysis of low-dimensional carbon nanostructures. He pioneered the use of thin layer electrochemistry for reducing diffusional limitations in ECs and multi-scale hierarchical charge storage.

Mark Hoefer
Program in Materials Science, Department
of Mechanical Engineering, University of
California, San Diego, La Jolla,
CA 92093-0411, USA

Mark Hoefer is presently a Research Engineer at Bosch, Germany. Mark graduated with a PhD from the University of California, San Diego, in 2012 with a thesis on the Electrochemical implications of defects in carbon nanostructures. He pioneered the harness of charged defects for controlled capacitive storage.